ISABE-2015- 20066

INVESTIGATION ON THE EFFECTS OF AN IMPROVED BLADE SURFACE PRESSURE DISTRIBUTION ON TURBINE BLADE TIP REGION LOSSES

Wei Zhao[1,2], Xiaorong Xiang [1,2], Qingjun Zhao [1,2], Jianzhong Xu[1]
1. Institute of Engineering Thermophysics, Chinese Academy of Sciences
2. Key Laboratory of Light-duty Gas-turbine, Institute of Engineering Thermophysics, Chinese Academy of Sciences
11 Beisihuanxi Road, Beijing 100190, People's Republic of China
zhaowei@iet.cn

Abstract

Turbine blade loading distributions at tip substantially affect the flow field inside the tip gap, the ejection of the tip leakage flow into the main stream and the formation of a leakage vortex in the blade passage. This paper presents an improved blade tip profile for a highly loaded transonic turbine to reduce the viscous losses related to the tip leakage vortex. The improved performance is explained by a close comparison of the flow fields of an original case and a redesigned case. Three dimensional steady-state viscous computations are conducted for the two cases to investigate the effect of blade tip profiles on the tip leakage flow to understand of the mechanisms responsible for the flow fields in blade tip regions. Turbulence is modeled using the two equation closure of SST for convergence. Two types of leakage vortex rollup mechanism are identified on a basis of the visualized leakage vortices for the two cases respectively. In the original case the fluid of the initial leakage vortex core mainly comes from the tip gap flow very near to the blade tip, and the convection of the vorticity generated in the tip gap is responsible for the formation of the leakage vortex core. In contrast, in the redesigned case the fluid of the leakage vortex core is entirely composed of the passage flow and the shearing of the leakage jet flow and passage flow leads to the formation of the leakage vortex. The different leakage vortex core formation mechanisms are attributed to the pressure distributions, or blade loadings, at blade tips for the two cases. The blade loading around 20% axial chord on the suction side is moved forward in the redesigned case, which makes the leakage flow in the tip gap near the leading edge leave the gap in a direction more normal to that of the passage flow. As a result, the shear stress between the pass flow and the leakage jet is increased. The increased shear stress helps the passage flow roll up into a leakage vortex core more easily. The redesigned tip profile noticeably reduces the losses and size of the leakage vortex because of the less vorticity transported in the vortex core. Although the shed vortex is enhanced due to the reduced blockage effects of the leakage flow on the passage vortex for the redesigned case, the total to total efficiency of the turbine rotor is increased by 0.20% due to the weakened leakage vortex.

Nomenclature

π	Pressure ratio
Ψ	Stage work Coefficient
Z	Axial Position normalized using blade axial chord

Introduction

A major aerodynamic loss in a turbine rotor is attributed to the formation and development of the tip clearance leakage vortex in the blade passage. The three dimension leakage flow interacts with not only the main stream but also the secondary flows as soon as it occurs, complicating the flow field in the blade tip region seriously. Therefore, most blade tip

designs do not seek to reduce the internal tip gap loss and leakage vortex mixing loss through detailed manipulation of the interacting flow and structures, but instead take the more straight forward approach of simply reducing the total tip leakage flow through sealing geometries and tight running clearances [1].

Since the pressure difference between the pressure and suction sides of a rotor blade is driving force that causes the undesirable leakage flow through the clearance gap, the blade pressure distributions would certainly affect the formation, development and diffusion of the leakage vortex. The effects of the leakage vortex on blade surface pressure distributions have been studied in numerous literatures, but rarely investigated were how blade surface pressure distributions influence the formation of the tip leakage vortex and what feature of a blade tip profile would aid to produce appropriate pressure distributions on the blade surface near tip to reduce the leakage flow losses.

The objective of this paper is to present a geometry improvement method for flatted turbine blade tips. This method adjusts the aerodynamic loading at the blade tip to affect the formation of the tip leakage vortex near the leading edge, as well as the development in the blade passage. The effects of the affected tip leakage vortex on the reduction in tip leakage flow losses are illustrated by detailed comparisons of the numerical results for the flow fields of an original case and a redesigned case.

Numerous investigations on turbine tip leakage flow physics and leakage vortex rollup mechanisms were conducted experimentally and numerically in the past decades. Sjolander and Amrud [2] conducted a turbine cascade experiment with surface oil flow visualization to gain insight into the tip leakage flow structure and its relationship with the blade loading near the tip. The leakage flow appeared to follow closely the direction of the maximum pressure gradient within the tip gap and began to roll up into a vortex after emerging from the gap. Multiple vortices were formed at the larger clearances and retained their identity resulting in multiple pressure peaks on the suction side of the turbine blade. Bindon [3] suggested that the major part of the gap loss arises when the slow-moving separation bubble flow is ejected from the low pressure zone in the gap by the high-speed leakage jet induced at midchord. Heyes and Hodson [4] concluded that the pressure gradient along the blade chord is a major factor influencing the tip leakage flow. They proposed a simple finite volume time-matching method, which relies on the knowledge of the pressure distribution at tip gap exit and on the blade pressure side away from the tip clearance, to predict the trajectories of the leakage streamlines. Xiao, et al. [5] experimentally observed the tip clearance flow originates near the mid-chord on the suction surface, interacts with the main stream and roll up into a leakage vortex with the highest total pressure loss. McCarter [6], et al. pointed out that the formation of the leakage vortex, its location and strength depend on the blade design pressure distribution and blade profile since the leakage flow tends to move toward the suction peak. Tallman and Lakshminarayana [7] performed CFD simulations that were validated by experimental measurements to understand the leakage flow and vortex physics in a turbine cascade. The leakage vortex roll-up due to the shearing of the leakage jet and passage flow was observed in none of the simulations. They found that the inner core of the leakage vortex was entirely composed of the fluid passing through the tip clearance gap from the leading edge and midchord near to the blade tip. When the casing relative motion was incorporated in the simulations [8], the mass flow of the tip clearance leakage was reduced and the size of the tip leakage vortex was smaller by the obstruction of the moving casing’s shear layer and the enhanced passage vortex. Krishnababu [9, 10] et al. numerically studied the effect of the flat tip geometry and

squealer type geometries on the tip leakage flow and heat transfer characteristics in an unshrouded axial flow turbine. The heat transfer and static distributions obtained using SST κ-ω turbulence flow model were found to be in close agreement with the experimental data. The cavity tip was advantageous both from aerodynamic and heat transfer perspectives because it achieved a decrease in the amount of leakage, losses, and heat transfer to the tip.

Blade Profile

The improvement method for turbine blade tip profiles is applied to a highly-loaded transonic turbine rotor with convergent blade passages, referred to as the original case. The effects of this method on reducing the tip leakage losses are demonstrated in a redesigned case. The primary parameters of the rotor blade are shown in Table 1.

The blade geometry is defined by 5 blade section profiles stacked at an almost equal spanwise interval from hub to tip along a straight line passing through the section gravity centers. In this study only the most outer blade section profile, that is, the blade tip profile is modified for the original case, leading to the redesigned case, as shown in Fig.1.

The redesign for the original case mainly lies in two aspects. First, the stagger angle of the blade tip section is increased by 3 degrees. In the same time the majority of the suction side curve is moved toward the camber line to maintain an unchanged throat width for a constant mass flow. Second, the pressure side curve near the leading edge is set to be a little more concave, or closer to the camber line.

The tip profile for the redesigned case appears to be thinner and the suction side curvature near the leading edge rises due to the increased stagger angle. In addition, the gravity center moves toward the trailing edge because most of the reduced area locates near the leading edge, so that the tip profile moves a little forward in the axial direction.

Table 1. Parameters of turbine blade

Tip clearance height to blade height, %	1.0
Stage work coefficient at meanline span, Ψ	2.8

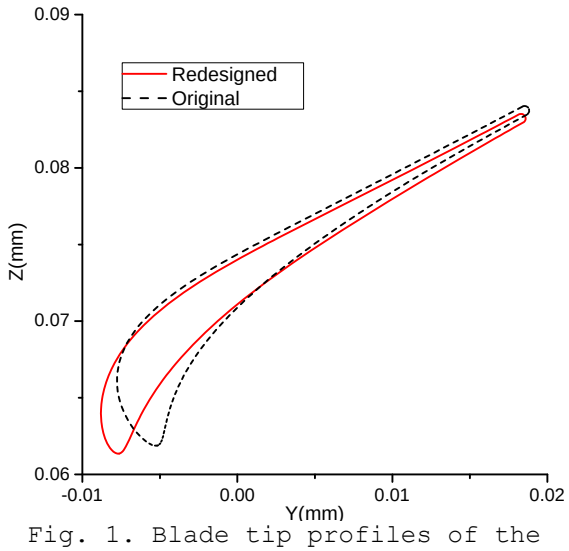

Fig. 1. Blade tip profiles of the original case and redesigned case

Numerical Simulation

Three dimensional steady-state viscous computations are carried out with the Fine/Turbo package of NUMECA to investigate the effect of blade tip section geometry on the tip leakage flow. The Reynolds Average Navier-Stokes equations are solved by using a finite volume method with central difference discretization and Runge-Kutta time marching approach. The boundary layer is supposed to be fully turbulent anywhere and the turbulence is modeled by the two equation closure of SST.

A structured mesh consisting of 2.1 million nodes and 12 blocks is used, as shown in Fig. 2. An O-grid is used around the blade and H-grids upstream of the leading edge, downstream of trailing edge, and in mid-passage. A total of 29 points is used normal to the blade profile in the O-grid. In the tip clearance region H-O-grid is used. The O-grid contains 21 points in the wraparound direction and 33 points

in the radial direction. The wall spacing is 1e-6m, which is small enough to resolve the boundary layer to obtain a maximum value of y+ less than 2.0 everywhere in the computational domain. Grid sensitivity is analyzed by comparing the solutions obtained with 2 million nodes and the solutions obtained with 3.2 million nodes for the original case. The prediction with these two grids yields similar results: the relative difference in total to total efficiency is found to be less than 0.01%, and the relative difference in mass flow rate less than 0.02%. Therefore, the mesh with 2.1 million nodes is suitable for the cases in this work.

Total pressure, total temperature and velocity vector distributions are specified at the inlet for boundary conditions according to the design valves from a throughflow calculation. The walls are assumed to be adiabatic. Radial equilibrium and a static back pressure are prescribed at the exit boundary.

Fig. 2. Mesh for CFD simulation

The numerical simulation results of the two cases, summarized in Table 2, show that the total to total efficiency of the redesigned case is improved by 0.2% at a nearly same working condition.

Table 2. Performance Comparison of the original case and redesigned case

	Original	Redesign-ed	%
Adiabatic efficiency	90.18	90.36	0.20
Mass flow rate, m/s	7.866	7.867	0.01
Stage pressure ratio	0.5019	0.5020	0.02

Flow Field Analysis

The performance differences between the two cases are directly related to their leakage vortex sizes. Entropy distributions at 105% axial chord for the original and redesigned cases are given in Fig. 3. A significant distinction observed in the redesigned case is that the leakage vortex creates a considerably smaller high entropy region than that in the original case. The width of the high entropy region in the original case is about 1.5 times than that in the redesigned case, and so it is with the leakage vortex core, implying that the leakage flow related losses is reduced in the redesigned case. Another noticeable entropy increasing region is under the leakage vortex roughly from 60% to 80% blade span in the wake, indicating that in this region the shed vortex, caused by the shearing of the secondary flow near the pressure side and the passage vortex near the suction side, is also enhanced. Since the entropy creation near the pressure side is nearly the same, the enhancement of the shed vortex can be attributed to a stronger passage vortex in that region. Nevertheless, the reduced losses due to the leakage flow is greater than the increased losses due to the enhanced shed vortex and passage vortex, so that the total to total efficiency of the redesigned rotor is still increased by 0.20%.

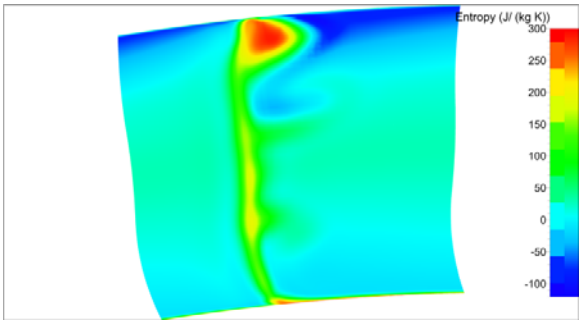

a) Original

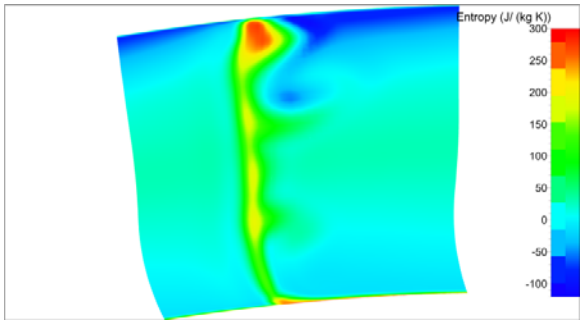

b) Redesigned

Fig. 3. Static entropy distributions at 105% axial chord for the original case and redesigned case

Fig. 4 shows the relative Mach number distributions at 95% span for the two cases. The flow fields share similarities in terms of the extent of the acceleration of the passage flow and the shape of the trailing edge shocks except for the width of the leakage flow in the blade passage. The edge of the leakage flow where it mixes with the passage flow in the original case is a little further from the suction side, especially near the trailing edge, implying that the leakage vortex is larger in size.

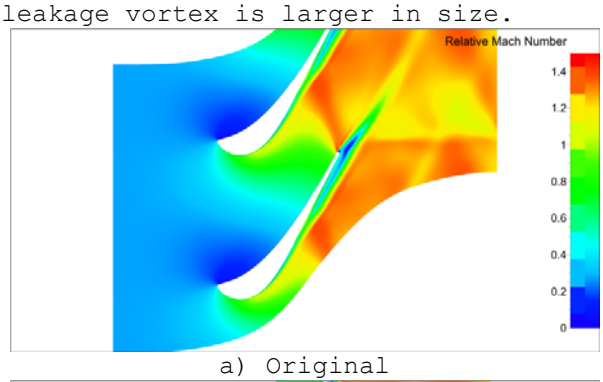

a) Original

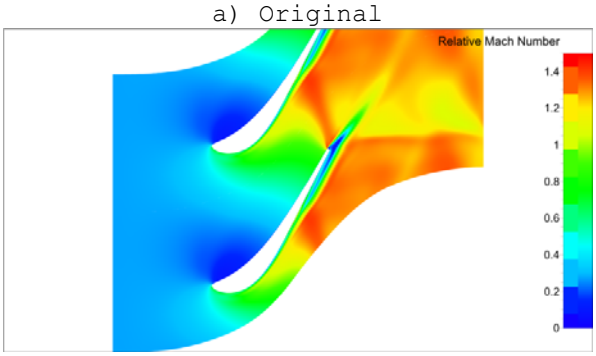

b) Redesigned

Fig. 4. Mach number distributions at 95% span for the original case and redesigned case

The leakage vortex core plays an important role in the development of the tip gap leakage flow in the blade passage, as well as the viscous losses generation in this process. Since the highest entropy in the blade tip region indicates the location of the leakage vortex core, 5 random points at 105% axial chord in that area are chosen for both cases to represent the locations where the inner part of the leakage vortex passes. The streamlines, or pathlines, which travel through these points, together with the entropy distribution at 105% axial chord, are plotted in the reference frame moving with the rotor blade in Fig. 5. These streamlines roll up with increasing radii as they move downstream in the blade passage, indicating the development of the leakage vortex clearly.

It should be remarked that no streamlines starting at the inlet of the calculation domain and ending in the highest entropy region of the blade passage exit could be generated for the original case, but such streamlines are present for the redesigned case. The streamlines in the original case, to some extent, are in similar situations observed by Tallman and Lakshminarayana [7, 8]. They concluded that the core of leakage vortex is rolled up due to vorticity convection and entirely composed of the fluid that passes through the tip clearance gap in the leading edge and midchord region. However, the streamlines in the redesigned case indicates another mechanism for the rollup of the leakage vortex. For the redesigned case the streamlines do not roll up into a leakage vortex until about 20% axial chord. Hence the rollup of the leakage vortex in the redesigned case can be attributed to the shearing of the leakage jet and passage flow since the leakage vortex in the forward part of the blade passage is composed of the fluid that is irrotational before meeting the leakage flow.

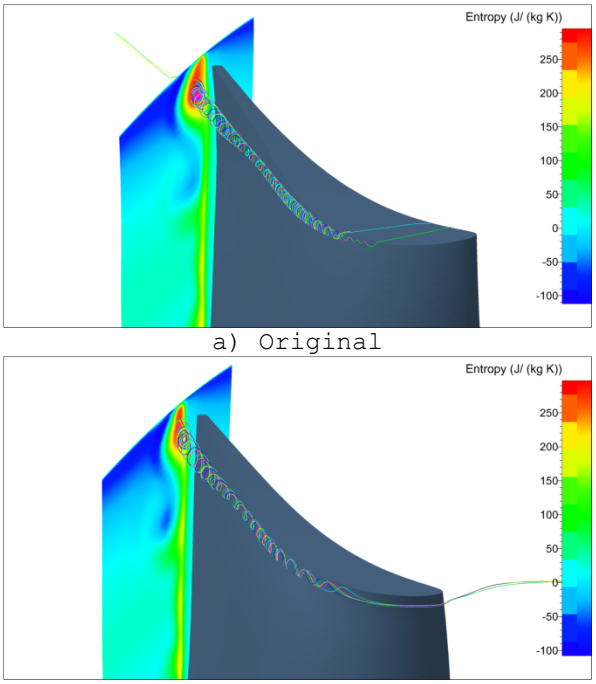

a) Original

b) Redesigned

Fig. 5. Streamlines passing through the tip leakage vortex for the original case and redesigned case

The rollup mechanism for the leakage vortex in the redesigned case is certainly related to its blade tip profile, which changes the pressure difference across the tip gap, the driving force that allows the leakage flow to pass through the blade tip gap. The static pressure distributions at 95% span of both cases are shown in Fig. 6.

Each case has an almost equal suction peak at the same axial position, but the static pressure distributions on the suction side from leading edge to 30% axial chord for the two cases differ substantially. A sharper drop in static pressure is observed at the leading edge for the redesigned case. Although the flows at 95% span are stagnated on the pressure side for both cases, the stagnation point for the redesigned case locates a little farther from the leading edge because of the increased stagger angle and the more concave pressure side near the leading edge. The longer distance the stagnated fluid has to travel before reaching the suction side results in a larger area contraction for the flow around the leading edge. Note that the flow there is subsonic, so the flow at the leading edge of the redesign case accelerates much faster toward the suction side and even overspeed occurs, resulting in a more dramatic static pressure drop at the leading edge.

The static pressure on the suction side of the redesigned case is greater between the leading edge and 9% axial chord, but smaller from 9% to 30% axial chord than that of the original case, indicating the blade loading is moved forward to the leading edge for the redesigned case. The increased stagger angle accounts for this pressure distribution difference, since a high stagger angle usually leads to a forward blade loading.

The pressure distributions on the pressure sides for both cases are nearly the same except for two minor differences. The stagnant point of the redesigned case results in a faster pressure drop on the pressure side near the leading edge. The more concave pressure side enlarges the passage width slightly and the flow on the pressure accelerates a little more slowly from the stagnant point to the trailing edge.

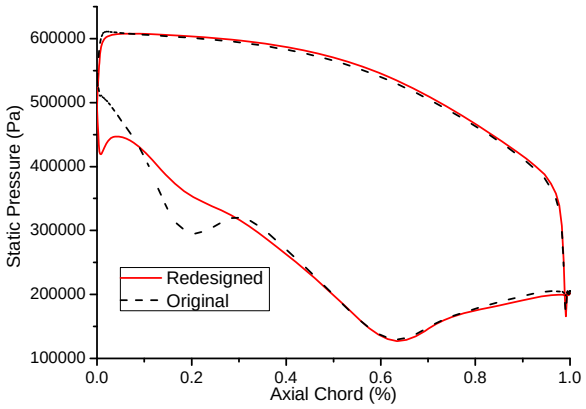

Fig. 6. Static pressure distribution on the blade surfaces at 95% span

The static pressure distribution of the redesigned case, especially on the suction side before 30% axial chord according to Fig. 6, must have a specific effect on the pathline of the tip leakage flow in the gap. Furthermore, the interaction of the

leakage jet and passage flow and the rollup mechanism for the leakage vortex are influenced consequently, as discussed below.

To compare the directions of the leakage flows in the tip gaps for the original and redesigned cases, the streamlines of the tip leakage flow about 5% blade tip gap span away from the blade tip between 2% and 99.5% axial chord are projected into the blade tip along the radial direction, as shown in Fig 7 a) and b).

In this perspective it is clear that for the original case the leakage flow near the leading edge passes through the tip clearance gap in a direction less normal to the suction side. This means that in the redesigned case the angles formed by the directions of the leakage flow and the passage flow are obviously greater. There are two factors responsible for the increased angle. On one hand, in the redesigned case the leakage flow in the tip gap near the leading edge can see lower pressures on the suction side from leading edge to 9% axial chord, as already shown in Fig. 6, moving toward the leading edge more easily. On the other hand, the increased stagger angle of the blade tip section for the redesigned case results in an earlier turning of the suction side near the leading edge, so that the direction of the suction side in that region is closer to the axial direction. Since both sides of the angle respectively revolve in opposite directions, the value of the angle is consequently enlarged.

Besides the direction in which the leakage flow ejects into the passage flow, the vorticity of the leakage flow also affects the interaction between the leakage flow and the passage flow, assisting in the formation mechanism for the leakage vortex and its rollup degree, as well as the associated viscous losses.

To illustrate the shearing effects due to the relative motion between the leakage jet and passage flow in the original case and redesigned case, the vorticity distributions in the tip leakage flow region are plotted at 25%, 40% , 85% and 105% axial chord respectively, as shown in Fig. 8.

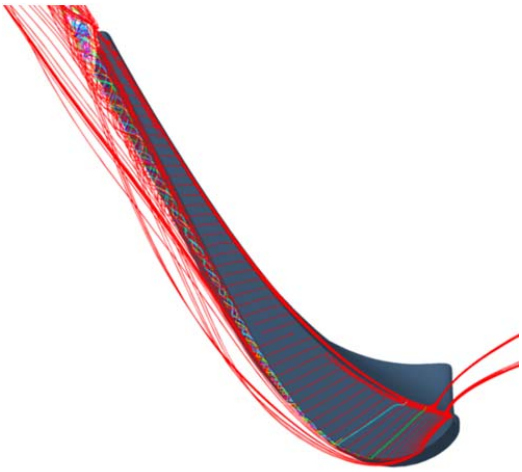

a) Original

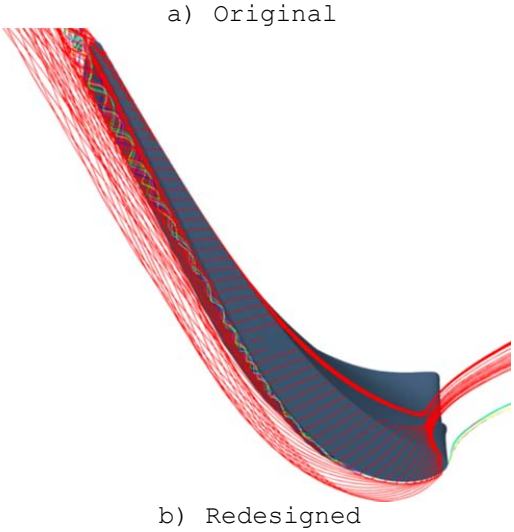

b) Redesigned

Fig. 7. Projection of the streamlines passing through the blade tip gap for the original case and redesigned case

The vorticity near the exit of the leakage gap at 25% axial chord of the redesigned case is apparently higher. This means the shearing of the leakage flow and the passage flow near the leading edge is stronger in the redesigned case, and a vortex rollup due to this shearing is more likely to take place in this region.

At 40% axial chord the vorticity in the corner between the suction side and the casing wall of the original case increases substantially when compared with the corresponding vorticity of the redesigned case, and

the high vorticity region confined closer to the suction surface indicates a weaker leakage jet.

At 80% axial chord the original case clearly shows a higher vorticity near the leakage vortex center. The vorticity variation of the inner part of the leakage vortex from 25% to 80% axial chord in the original case indicates the presence of the vorticity convection from the tip gap. As the leakage vortex rolls up, the leakage vortex core comprises the fluid passing through the tip gap with high vorticity, as shown in Fig. 5 a), so that the vorticity in the inner part of the leakage vortex becomes greater.

At 105% axial chord the high vorticity region in the leakage vortex for the original case, with values greater than 3E6, is about 1.5 times larger in width than that for the redesigned case, but the maximum values in the center of this region is about 20% lower. This difference regarding vorticity distribution in this area rises from the diffusion of the leakage vortex. The leakage vortex of the original case with greater vorticity dissipates much more easily or even tends to break down in the diffusion region beyond 65% axial chord, as shown in Fig.6, so the region of the leakage vortex downstream of the trailing edge becomes more uniform in vorticity but larger in size. Moreover, the passage vortex near casing in the redesigned case undergoes a less obstruction due to the smaller leakage vortex, so the shed vortex caused by the shearing between the outward secondary flow on the pressure side and the inward passage vortex on the suction side, is stronger in the wake.

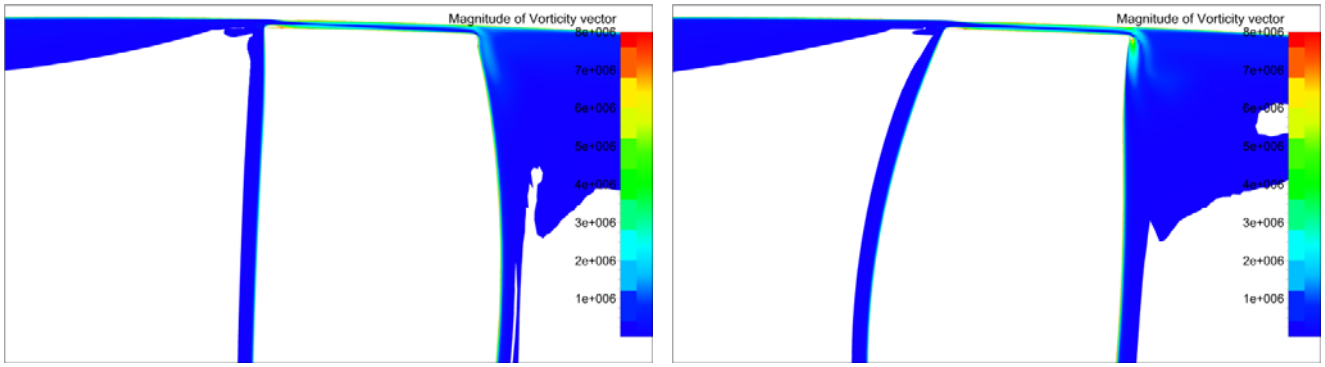

a) 25% axial chord

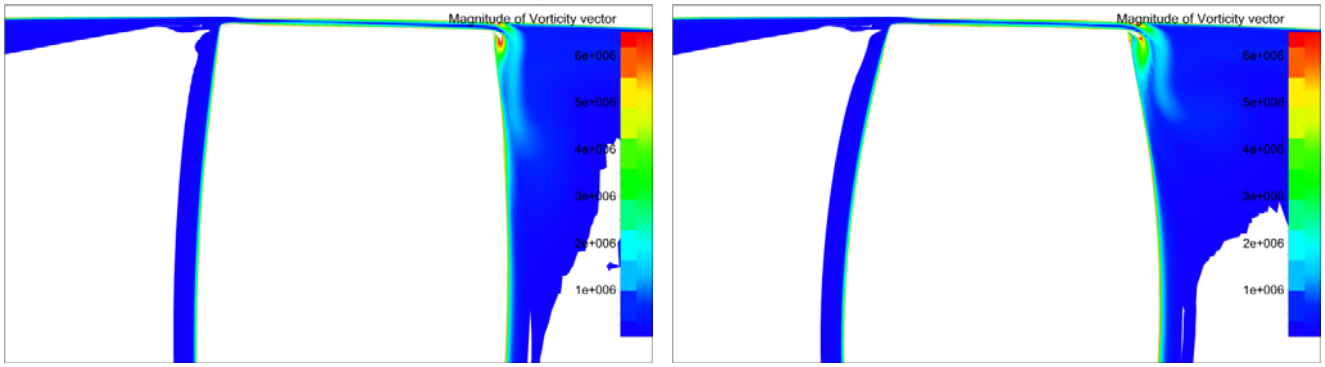

b) 40% axial chord

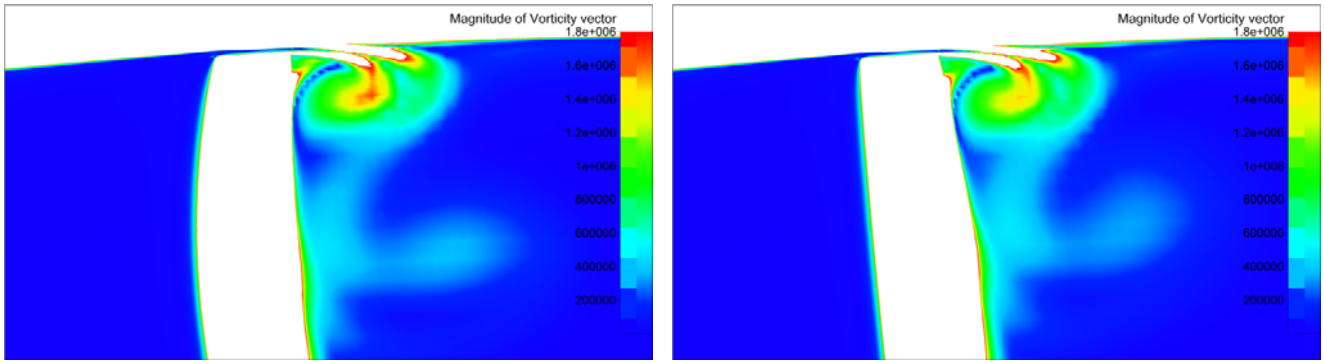

c) 80% axial chord

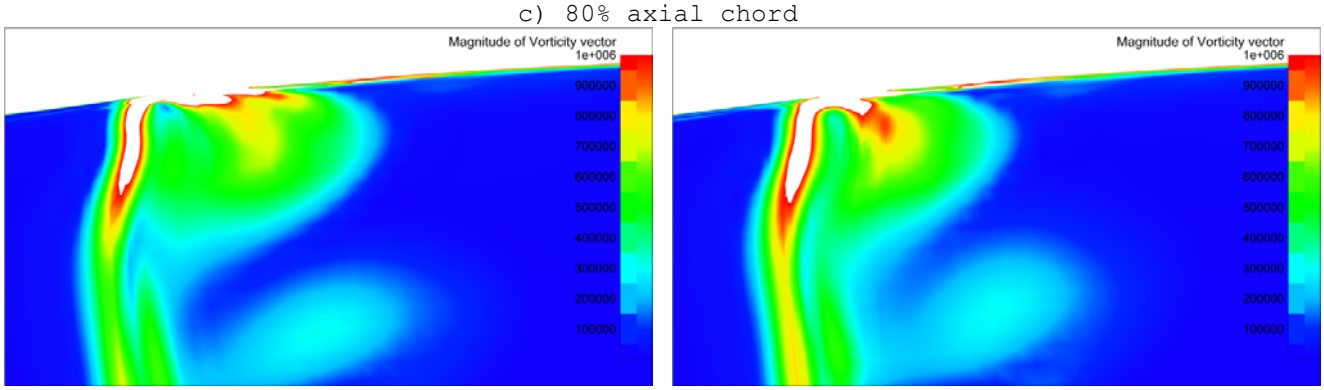

d) 105% axial chord

Fig. 8. Vorticity distribution in blade tip region at 25%, 40%, 85% and 105% axial chord
(Left: the original case; Right: the redesigned case

Based on the described above on the flow fields in the tip gaps and the shearing of the leakage flow and passage flow, two types of leakage vortex formation mechanisms account for the differentials between the original case and the redesigned case.

The velocity vector of the tip leakage jet at the exit of the tip gap can be decomposed into two components. One is in the passage flow direction and the other in the direction normal to the passage flow. According to triangle relationships, the larger the angle formed by the directions of the leakage jet and passage flow is, the greater the velocity component of the leakage jet which is normal to the passage flow would be. Since such an angle is increased in the redesigned case, greater shearing stress and vorticity are present as shown in Fig. 8 a). With the increased shearing the leakage flow of the redesigned case rolls up the passage flow into a leakage vortex near the leading edge, which is referred to as a shearing mechanism. Once the leakage vortex is formed in the blade passage, the downstream leakage jet gap wrap around the external part of the leakage vortex, rather than enter the inner part. As a result, no high vorticity of the leakage flow generated in the tip gap can be transported into the leakage vortex. Therefore the viscous losses in the redesigned case generated in the leakage vortex are relatively lower. On the contrary the leakage flow at the exit of the tip gap in the original case is at a smaller angel with the passage flow. The rollup of the leakage vortex, which is made up of the fluid from the tip gap, is attributed to the vorticity convection from the gap instead of the weakened shearing of the leakage jet and the passage flow, referred to as a convection mechanism. The leakage vortex formed in this manner is greater in size and loss due

to the dissipation related to the high vorticity in it.

Conclusion

This paper presents an improved blade tip profile for a highly loaded transonic turbine rotor, as well as its effects on the formation and loss of the tip leakage vortex. This paper also numerically demonstrates for the first time that leakage vortex formation mechanisms can be related to blade tip profiles and the associated pressure distributions on the blade surface at tip. The main conclusions of the current study are as follows:

1. Turbine blade tip profiles that adjust the pressure distributions on the blade surface at tip, especially on the suction side, are able to affect the mechanism for the formation of a leakage vortex, the associated viscous losses and the blockage effect of the leakage flow on the secondary flow. A blade tip profile with increased loading near the leading edge tends to cause the rollup of a leakage vortex by the shearing of the leakage jet and passage flow, referred to as a shearing mechanism. Meanwhile a blade tip profile with decreased loading near the leading edge results in the rollup of a leakage vortex due to the vorticity convection of the leakage flow from the tip gap, referred to as a vorticity convection mechanism.

2. The shearing mechanism is present because the leakage flow leaves the tip gap in a direction more normal to the direction of the passage flow. The strong shearing between them aids in the rollup of the passage flow into a leakage vortex. As to the vorticity convection mechanism, the shearing between the leakage flow and the passage flow is relatively weak due to the smaller angle formed by their directions. The leakage vortex in blade passage does not occur until the tip leakage flow passes a distance on the blade tip long enough to generate sufficient vorticity in it. The rotational fluid itself then rolls up into a leakage vortex with the high vorticity transported from the tip gap.

3. The inner part of the leakage vortex formed with the vorticity convection mechanism contains the fluid from the tip gap with high vorticity, while that formed with the shearing mechanism is entirely composed of the passage flow that is initially irrotational. The tip gap flow induces a higher vorticity to the leakage vortex, resulting in greater entropy generated in the vortex dissipation process and a larger size of the leakage vortex at the exit of the blade passage. Due to the reduced losses associated with the leakage vortex, the shearing mechanism improves the efficiency of the turbine rotor.

Acknowledgment

This study was supported by National Natural Science Foundation of China (No. 51006098).

References

[1] Bunker RS. Axial Turbine Blade Tips: Function, Design, and Durability. Journal of Propulsion and Power. 2006;22(2):271-285.doi: 10.2514/1.11818

[2] Sjolander SA, Amrud KK. Effects of Tip Clearance on Blade Loading in a Planar Cascade of Turbine Blades. ASME. J. Turbomach.. 1987;109(2):237-244. doi:10.1115/1.3262090.

[3] Bindon JP. The Measurement and Formation of Tip Clearance Loss. ASME. J. Turbomach.. 1989;111(3):257-263. doi:10.1115/1.3262264.

[4] Heyes FG, Hodson HP. Measurement and Prediction of Tip Clearance Flow in Linear Turbine Cascades. ASME. J. Turbomach.. 1993;115(3):376-382. doi:10.1115/1.2929264.

[5] Xiao X, McCarter AA, Lakshminarayana B. Tip Clearance Effects in a Turbine Rotor: Part I—Pressure Field and Loss. ASME. J. Turbomach.. 2000;123(2):296-304. doi:10.1115/1.1368365.

[6] McCarter AA, Xiao X, Lakshminarayana B. Tip Clearance Effects in a Turbine Rotor: Part II—Velocity Field and Flow Physics. ASME. J. Turbomach.. 2000;123(2):305-313. doi:10.1115/1.1368880.

[7] Tallman JJ, Lakshminarayana BB. Numerical Simulation of Tip Leakage Flows in Axial Flow Turbines, With Emphasis on Flow Physics: Part I—Effect of Tip Clearance Height. ASME. J. Turbomach.. 2000;123(2):314-323. doi:10.1115/1.1368881.

[8] Tallman JJ, Lakshminarayana BB. Numerical Simulation of Tip Leakage Flows in Axial Flow Turbines, With Emphasis on Flow Physics: Part II—Effect of Outer Casing Relative Motion. ASME. J. Turbomach.. 2000;123(2):324-333. doi:10.1115/1.1369113.

[9] Krishnababu SK, Newton PJ, Dawes WN, et al. Aerothermal Investigations of Tip Leakage Flow in Axial Flow Turbines—Part I: Effect of Tip Geometry and Tip Clearance Gap. ASME. J. Turbomach.. 2008;131(1):011006-011006-14. doi:10.1115/1.2950068.

[10] Krishnababu SK, Dawes WN, Hodson HP, Lock GD, Hannis JJ, Whitney CC. Aerothermal Investigations of Tip Leakage Flow in Axial Flow Turbines—Part II: Effect of Relative Casing Motion. ASME. J. Turbomach.. 2008;131(1):011007-011007-10. doi:10.1115/1.2952378.